

Constraining Electron's Parallel Energy in Electrostatic Field through Anomalous Doppler Effect Induced by External Electromagnetic Waves

A. Author,^{1, a)} B. Author*,¹ and C. Author^{2, b)}

¹⁾Authors' institution and/or address

²⁾Second institution and/or address

(*Electronic mail: Second.Author@institution.edu.)

(Dated: 22 December 2024)

In this study, the interaction between free electrons and ElectroMagnetic Waves (EMW) in the presence of magnetic and electrostatic fields is simulated using the Volume-Preserving algorithm. We found that when the electric field of the EMW (which includes a left-hand polarization component) exceeds a critical value, it can continuously transfer the electron's parallel energy into rotational energy via the Anomalous Doppler Effect (ADE). This mechanism converts the work by the electric field along the background magnetic field into perpendicular kinetic energy. As a result, the electron's parallel kinetic energy saturates, while its perpendicular kinetic energy increases continuously. The model based on energy, momentum, and angular momentum conservation is given to provide a clear explanation of the contribution of left-hand polarization to the Anomalous Doppler Effect. This general model can be directly applied to interpret the anomalous Doppler effect in electron-wave interaction. To saturate the parallel energy of runaway electrons in magnetically confined plasma, we propose an innovative solution for runaway electron mitigation in Tokamaks by launching extraordinary wave from the high-field side with an energy flux of several watts per square meter.

I. INTRODUCTION

During the current ramp-up phase in tokamak, disruptions or magnetohydrodynamic (MHD) instabilities can induce quasi-static toroidal electric field, which accelerates electrons to energies on the order of several tens of MeV. This acceleration occurs when the force from the quasi-static electric field exceeds the drag from radiation and collisions. The accelerated electrons, known as runaway electrons, can cause significant damage to the interior walls of the device, thereby reducing its operational lifespan. It is worth considering the possibility of converting the acceleration of electrons from quasi-static electric field into rotational energy within magnetic field. This conversion not only suppresses the energy of runaway electrons, mitigating their detrimental effects on the device, but also enhances discharge performance by reducing the consumption of ohmic field energy. The transport of parallel energy in electrons to rotational energy primarily occurs through three mechanisms: electron avalanche processes¹, collisionless pitch-angle scattering², and the Anomalous Doppler effect (ADE)³. The first two methods to suppress runaway processes, such as gas injection⁴ and enhancing magnetic perturbations⁵, usually have side effects and alter the discharge environment. In contrast, the latter method can be a clean process, making it particularly attractive for investigation.

When electrons move in static magnetic field and interact with external electromagnetic wave (EMW) with frequency ω and wave vector \vec{k} , they experience a scattering phenomenon under the resonant condition $\omega - \vec{k} \cdot \vec{v} = n\omega_{ce}$, where $n > 0$ and $\omega_{ce} > 0$. The result of this scattering is a transfer of momentum from parallel motion to rotational motion, a phenomenon

known as the Anomalous Doppler Effect. This effect was thoroughly described in the classic works of Ginzburg and Frank^{3,6,7}. Recently ADE has raised increasing attentions in space radiation⁸, runaway electron instability⁹ and materials science¹⁰, it is believed that ADE can explain the phenomena as whistler turbulence in flare loops⁸, the Electron Cyclotron Emission (ECE) with step-like structure in Tokamak¹¹⁻¹³ and the microwave bursts during Edge Localized Modes (ELM)¹⁴. Additionally, ADE holds potential for suppressing runaway electron energy in Tokamak discharges. This has been demonstrated by F. Santini, who found that high-energy runaways can be significantly reduced through ADE during lower hybrid waves heating in the Frascati Tokamak¹⁵. However, it is important to note that the high power of lower hybrid waves also causes an increase in nonthermal electrons through Landau resonance. This, in turn, leads to an increase in runaway electrons after shutdown of lower hybrid waves, which is a side effect of using lower hybrid waves to suppress runaway electrons.

Despite the Anomalous Doppler Effect (ADE) having been described in numerous experiments and theories¹⁶⁻²⁴, previous descriptions of the single-particle ADE have mainly relied on either quantum theory or classical theory, disregarding the accelerating electrostatic field^{15,25,26}. Further exploration of the ADE in the presence of electrostatic field is essential for understanding the physics of pitch-angle scattering of runaway electrons by electromagnetic waves in Tokamak discharges. Moreover, the nature of ADE in classical electrodynamics fields remains unclear due to the complexity of formulas in previous classical theories. For instance, it is still difficult to understand why parallel kinetic energy can convert to transverse internal energy during ADE resonance, or what kind of ElectroMagnetic Waves (EMW) can trigger ADE. These questions require further investigation.

This paper directly simulates the full orbit electron motion in uniform magnetic field with accelerating electrostatic

^{a)} Also at Physics Department, XYZ University.

^{b)} <http://www.Second.institution.edu/~Charlie.Author>.

field and electromagnetic field using the Volume-Preserving Algorithm²⁷. Compared to conventional algorithms, such as Boris, Volume-Preserving Algorithm can acquire long-term accuracy and conservativeness via a systematic splitting method, which is an excellent method for nonlinear electron dynamic simulation. To directly demonstrate the phenomenon of the ADE, we place an electron in uniform magnetic field B_0 along with electrostatic field E_0 that is oriented in the opposite direction to B_0 . As a result, the electron can be accelerated parallel to B_0 . Additionally, during the simulation, the slow electromagnetic wave with its phase velocity smaller than that of light in vacuum is set up as induced wave. This induced wave allows us to directly observe the effects when the electron's velocity reaches the resonant condition for the ADE. We explore the resonance with three types of polarization waves including linear polarization, left-hand circular polarization and right-hand circular polarization in the simulation. We find only the wave with left-hand circular polarization can have ADE for runaway electron. The critical energy of wave when the electron parallel velocity can be constrained and consistently transport the parallel energy from electrostatic field to transverse rotation energy is also found in the simulation. Plus, the self-consistency between the quantum theory and direct simulation about ADE is examined. Finally, after analysing dispersion, polarization, and resonant moment, we have determined that the extraordinary wave is the most suitable for triggering ADE in plasma. Based on these findings, we propose a promising method for controlling runaway electrons.

II. QUANTUM THEORY OF ADE

This extraordinary phenomenon has already been discussed from energy conservation in the works of V.L.Ginzburg²³, I. Tamm²⁸, Nezlin⁷ and I.M.Frank²⁹. Here we give an analysis based on the conservation of angular momentum.

As shown in Fig. 1, When charged particles move through a medium faster than the speed of light in the medium, induced currents are generated. These currents stimulate secondary waves that interfere with the electromagnetic field of the particles in motion, thus giving rise to Cherenkov radiation. The direction of Cherenkov radiation can only be along the Cherenkov radiation angle $\theta_0 = \arccos(\frac{c'}{v})$, where c' is the speed of light in the medium and v is the velocity of charge particles. Now let's substitute the charge particle with a system that has internal energy (for example a oscillator or a cyclotron electron in magnetic field). The system moving faster than the speed of light ($v > c'$) emits photons with angular frequency ω and wavevector k at direction θ , where direction of the photon performs not depend on the interference of the secondary waves and can be in any direction, as shown in Fig. 2. According to energy conservation and moment conservation, we have :

$$T_1 + U_1 = \hbar\omega + T_2 + U_2 \quad (1)$$

$$\mathbf{p}_1 = \mathbf{p}_2 + \hbar\mathbf{k} \quad (2)$$

Where T_1 and U_1 represent the kinetic energy and internal

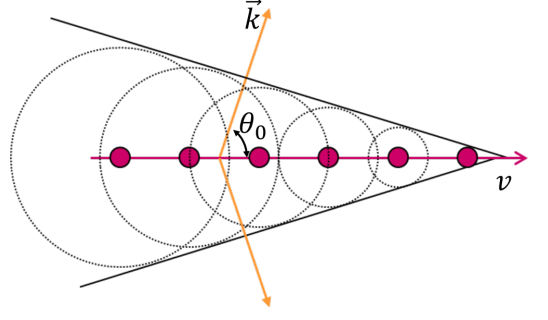


FIG. 1. Schematic diagram Cherenkov Radiation, the red point is the snapshot of the electron at different times

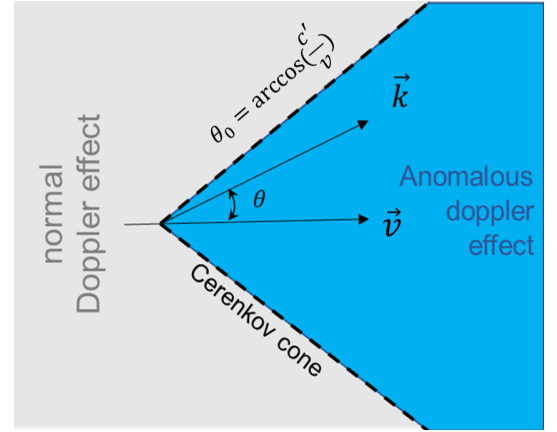


FIG. 2. The region of ADE ,Normal Doppler Effect (NDE) and Cherenkov cone, where the blue region refer to ADE, gray region refer to NDE while the dot line refer to the Cerenkov cone¹⁰

energy of system before emitting photon, T_2 and U_2 represent energy of system after emitting photon. Considering the photons energy far less than the initial kinetic energy T_1 , the loss of kinetic energy after emitting a photon can be expressed as $\Delta T_{12} = T_1 - T_2 = \Delta \mathbf{p} \cdot \mathbf{v}$, where \mathbf{v} is the velocity of system before emitting photon, also $\Delta \mathbf{p} = \mathbf{p}_1 - \mathbf{p}_2 = \hbar\mathbf{k}$. According to Eq. (1-2), we have :

$$\begin{aligned} \Delta U_{21} &= \Delta T_{12} - \hbar\omega \\ &= \hbar\mathbf{k} \cdot \mathbf{v} - \hbar\omega \\ &= \hbar\omega \left(\frac{kv \cos \theta}{\omega} - 1 \right) \end{aligned} \quad (3)$$

Here $\omega/k = c'$, $\Delta U_{21} = U_2 - U_1$. While the system velocity is more than the speed of light in the medium ($v > c'$), according to the sign of ΔU_{21} , we can divide radiation into three regions, as shown in Fig. 1 : For $\theta > \theta_0$ ($\cos \theta_0 = \frac{c'}{v}$), $\Delta U_{21} < 0$, The system produces photons by consuming its own internal and kinetic energy, this region refer to Normal Doppler Effect (NDE); For $\theta < \theta_0$, $\Delta U_{21} > 0$, this region refer to Anomalous Doppler Effect (ADE), where the system gains internal energy after emitting photons. It means the loss of kinetic energy is converted to photons and the system's internal energy; For $\theta = \theta_0$, $\Delta U_{21} = 0$, The loss of kinetic

energy by the system is completely converted into photon energy, this line refers to Cerenkov Effect(CE). All three effects are possible when the system velocity exceeds the speed of light ($v > c'$). While the system velocity is less than the speed of light ($v < c'$), only NDE exit. As we can see, we can judge the type of phenomena based on the change of internal energy after emitting photons.

Now consider the particular case in which the system is a electron moving freely with velocity v_z in the direction of external magnetic field $B = B_z$ and having small transverse ($\perp B$) velocity component v_\perp , then the kinetic energy of the cyclotron electron could be expressed as $T = \gamma m_e c^2 - m_e c^2$ and the internal energy represents as $U = \frac{1}{2} \gamma m_e v_\perp^2$, which is the equal to rotational energy of the electron as shown in Fig. 3. Here the γ refers to is Lorentz factor. In order to calculate the change of rotational energy, we should combine with another conservation: The angular momentum conservation, where:

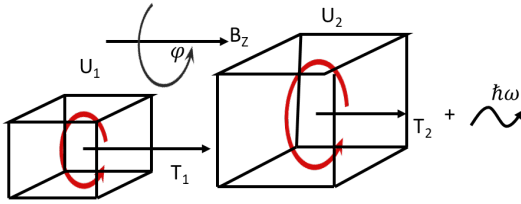


FIG. 3. Schematic diagram of electron cyclotron system, here $U_2 > U_1$, $T_2 < T_1$

$$L_1 = L_2 + n\hbar \quad (4)$$

Here we consider that the emitted photon contains angular moment with $n\hbar$ and the angular momentum of cyclotron electron before and after emitting photon is L_1 and L_2 , since the magnetic field is along the z direction, L should be equal to L_z . From the quantum theory, the electron wave in static magnetic field can be expressed as:

$$\Psi = \Psi_0 e^{\frac{i}{\hbar}(\mathbf{p} - e\mathbf{A}) \cdot \mathbf{s}} \quad (5)$$

where the Ψ_0 is normalized coefficient, \mathbf{A} is vector potential and \mathbf{s} is the position. The intrinsic equation of angular moment in z direction is :

$$-i\hbar \frac{\partial}{\partial \varphi} \Psi = (\mathbf{p}_\varphi - e\mathbf{A}_\varphi) r \Psi \quad (6)$$

the eigenvalue of L_z is:

$$L_z = (\mathbf{p}_\varphi - e\mathbf{A}_\varphi) r \quad (7)$$

consider $p_\varphi = \gamma m_e v_\perp$, $A_\varphi = \frac{rB_0}{2}$, and $r = \frac{\gamma m_e v_\perp}{B_0 e}$, we have :

$$L_z = \frac{1}{2} \frac{\gamma m_e v_\perp^2}{\omega_{ce}} = \frac{U}{\omega_{ce}}, \omega_{ce} = \frac{eB}{m_e \gamma} = \frac{\omega_0}{\gamma} \quad (8)$$

where m_e is the rest mass of electron, γ is Lorentz factor and ω_0 is electron cyclotron frequency in rest frame. The variation in the angular momentum of the electron along z is :

$$\Delta L_{21} = L_{z2} - L_{z1} = \frac{U_2 - U_1}{\omega_{ce}} = m\hbar \quad (9)$$

where m is the number of photon's angular momentum in z direction, than we have :

$$\Delta U_{21} = m\hbar \omega_{ce} \quad (10)$$

According to Eq. (3) and Eq. (10), we have :

$$\hbar \vec{k} \cdot \vec{v} = \hbar \omega + m\hbar \omega_{ce} \quad (11)$$

or

$$\omega = k_z v_z - m\omega_{ce} \quad (12)$$

Here, $\hbar \vec{k} \cdot \vec{v}$ represents the loss of kinetic energy ΔT_{21} , $\hbar \omega$ represents the energy of the photon, and $m\hbar \omega_{ce}$ represents the change in electron cyclotron energy ΔU_{21} (also called the change in internal energy). There are three situations for ΔU_{21} :

1. When $m < 0$, $\Delta U_{21} < 0$, the cyclotron electron internal energy decreases after emitting photon, and the emitted photon will have right-hand circular polarization with angular momentum $m\hbar$ to maintain angular momentum conservation. This process is called the Normal Doppler Effect.
2. For $m = 0$, $\Delta U_{21} = 0$, the Cherenkov Effect occurs, where the emitted photon does not cause any change in the internal energy of the cyclotron electron.
3. When $m > 0$, $\Delta U_{21} > 0$, the Anomalous Doppler Effect (ADE) occurs, resulting in an increase in the internal energy of the cyclotron electron and the emission of left-hand circular polarization with angular momentum $-m\hbar$.

As a result, the resonant condition is strongly associated with the wave's angular momentum. For a plane wave, the wave angular moment number includes only $m = \pm 1$. While for $|m| > 1$, it indicates that the resonant wave possesses a helicon structure. Based on above discussion, there are three kinds of resonant for system when electron moves along the uniform magnetic field with velocity v under external EMW, the resonant frequencies are Normal Doppler frequency (ω_{NDE}), Cerenkov frequency ($\omega_{Cerenkov}$), and anomalous Doppler frequency (ω_{ADE}). We only include $m = 0, \pm 1$ assuming they are the most dominant resonances, than these frequencies are respectively :

$$\omega_{NDE} = kv_z \cos \theta + \omega_{ce} \quad (13)$$

$$\omega_{Cerenkov} = kv_z \cos \theta \quad (14)$$

$$\omega_{ADE} = kv_z \cos \theta - \omega_{ce} \quad (15)$$

where θ is the angle between \vec{B} and \vec{k} . This equations are quite common resonant conditions for the kinetic equation of plasma ,what is intriguing is how the motion of electrons differs under various resonant conditions with electrostatic field. However, this aspect has been far less researched in recent years.

III. SIMULATION FRAMEWORK

Considering uniform magnetic field \vec{B}_0 in the z direction, the electron is accelerated in the \vec{B}_0 field by electrostatic field \vec{E}_0 that has opposite direction to \vec{B}_0 as shown in Fig. 4. To

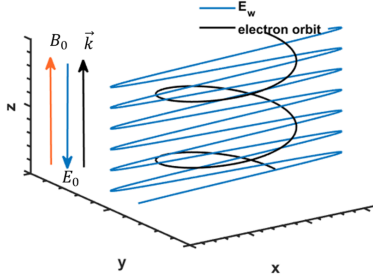


FIG. 4. Scheme of simulation setup

analyze the dynamics of electrons during interactions with electromagnetic field, we establish plane EMW characterized by frequency ω and wavevector \vec{k} . The angle between \vec{k} and \vec{B}_0 is denoted as θ , the equation of motion of the electron is :

$$\begin{aligned} \frac{d\mathbf{x}}{dt} &= \frac{\mathbf{p}}{\sqrt{m_0^2 + \mathbf{p}^2/c^2}} \\ \frac{d\mathbf{p}}{dt} &= q \left(\mathbf{E}(\mathbf{x}, t) + \frac{\mathbf{p}}{\sqrt{m_0^2 + \mathbf{p}^2/c^2}} \times \mathbf{B}(\mathbf{x}, t) \right) \end{aligned} \quad (16)$$

Here \vec{E} and \vec{B} is the sum of static field and EMW field. By using VPA algorithm^{27,30,31}, the discrete structure of differential Eq. (16) can be written as :

$$\begin{cases} \mathbf{x}_{k+\frac{1}{2}}^* = \mathbf{x}_k^* + \frac{\Delta t^*}{2} \frac{\mathbf{p}_k^*}{\gamma_k}, \\ \mathbf{p}^{*-} = \mathbf{p}_k^* + \frac{\Delta t^*}{2} \mathbf{E}_{k+\frac{1}{2}}^*, \\ \mathbf{p}^{*+} = \text{Cay} \left(\frac{\Delta t^* \mathbf{B}^*}{2\gamma^{*-}} \right) \mathbf{p}^{*-}, \\ \mathbf{p}_{k+1}^* = \mathbf{p}^{*+} + \frac{\Delta t^*}{2} \mathbf{E}_{k+\frac{1}{2}}^*, \\ \mathbf{x}_{k+1}^* = \mathbf{x}_{k+\frac{1}{2}}^* + \frac{\Delta t^*}{2} \frac{\mathbf{p}_{k+1}^*}{\gamma_{k+1}}, \end{cases} \quad (17)$$

The operator $\text{Cay}(A)$ denotes the Cayley transform of matrix A ²⁷, the dimensionless magnetic matrix \hat{B}^* is :

$$\hat{B}^* = \begin{pmatrix} 0 & B_z^* & -B_y^* \\ -B_z^* & 0 & B_x^* \\ B_y^* & -B_x^* & 0 \end{pmatrix} \quad (18)$$

The dimensionless parameters are momentum $p^* = \frac{p}{m_e c}$, magnetic field $B^* = B / \frac{m_e}{e \tau_{ce}}$, total electric field $E^* = E / \frac{m_e c}{e \tau_{ce}}$,

time step $\Delta t^* = \frac{\Delta t}{\tau_{ce}}$, and position $x^* = \frac{x}{\tau_{ce} c}$ respectively, where the τ_{ce} is electron cyclotron period and $\gamma^* = \sqrt{1 + p^{*2}}$.

We start with linearly polarized wave with direction $\theta = 0^\circ$. To reduce the simulation time, B_0 is set to 2×10^{-2} T. The wave angle frequency is $\omega_s = 1.5 \omega_0$, where $\omega_0 = \frac{e B_0}{m_e}$. The wavevector \vec{k} is parallel to z and $k = 10^5/\text{m}$. The amplitude of the electric field of the electromagnetic wave is $E_S = 9 \text{ V/m}$ and the electrostatic field is $E_0 = -2.5 \text{ V}$. All this parameters are set without reality consideration ,merely for quick simulation . The time step always satisfies $\Delta t = \min \left(\frac{2\pi}{50(k \cdot \vec{v})}, \frac{2\pi}{50\omega}, \frac{2\pi}{50\omega_0} \right)$ to ensure the accuracy of the simulation. The electron starts off stationary but gradually gains speed . Simultaneously, the resonant

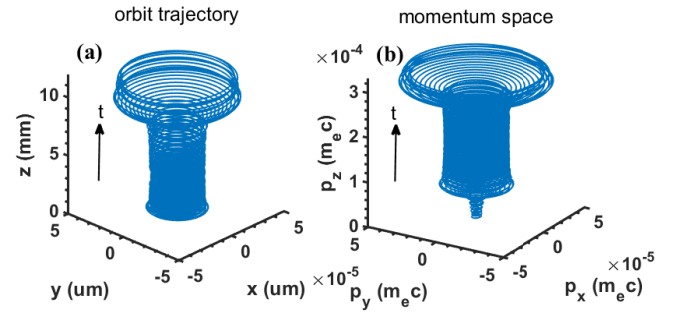


FIG. 5. (a) Orbit trajectory of electron motion (b) Momentum phase space of electron motion

frequency increases according to Eq. (13-15). Fig. 5 shows the evolutions of the electron's orbit and velocity phase during acceleration. The details of the electron's motion are given in Fig. 6. The resonant frequencies increase simultaneously (Fig. 6(a)) during electron acceleration in the electrostatic field (Fig. 6 (b)). When the Normal Doppler frequency equals to induced wave at about $23\tau_{ce}$, the perpendicular velocity (or rotational velocity) v_\perp quickly grow up (Fig. 6(d)). The parallel velocity v_z caused by EMW also increases simultaneously , as shown in Fig. 6(c), which can be calculated from $\Delta v_z = v_z - v_{zE0}$ where v_z is the parallel velocity in EMW and electrostatic field while v_{zE0} is only the result of electrostatic field . This phenomenon represents NDE where the resonant velocity $v_{NDE} = (\omega - \omega_{ce})/k_z < c'$ is "subluminal". The absorption of induced waves by the cyclotron electron causes an increase of velocity in parallel and perpendicular directions which can be viewed as a reverse process for system emitting photon as discussed before (The NDE process is widely used for in current drive³² and plasma heating³³ in Tokamak , although it is generally believed that the current drive by electromagnetic waves follows the Fisch mechanism³⁴ due to the limited toroidal moment injected by the waves). However, the resonant condition is quickly broken as the parallel velocity keep increasing until it reaches $v_{ADE} = \frac{\omega + \omega_{ce}}{k_z}$, at which point the ADE starts to come into view. When time arrives at $113 \tau_{ce}$, the system

starts to resonant with induced wave through ADE, where the $\omega_{ADE} = \omega$ as shown in Fig. 6(b), the parallel velocity begins to scatter to perpendicular direction as we can see the decrease of Δv_z and the increase of v_\perp shown in Fig. 6(c) and Fig. 6(d). The resonant condition quickly disappears as the parallel velocity surpasses the resonant region. To determine which type of ElectroMagnetic Waves is responsible for the NDE and ADE separately, we separate the linear polarized wave into left-handed circular polarization and right-handed circular polarization. We observe that the right-hand circular polarized wave is responsible for the NDE, while the left-hand circular polarized wave induces the ADE, as illustrated in Fig. 6(e) which agree well with our previous analysis. We can understand this phenomenon through the conservation of angular momentum and momentum: Because electron have a right-hand spin orbital angular momentum in a magnetic field, when electron absorb right-handed electromagnetic waves propagating in the parallel direction, according to the conservation of momentum and angular momentum, the parallel momentum and rotational energy of the electron will also increase, this process corresponds to NDE. When the electron emit left-hand circular electromagnetic waves propagating in the parallel direction, the conservation of momentum results in a decrease in the electron's parallel momentum, while the conservation of angular momentum requires an increase in the electron's rotational energy, this process corresponds to ADE. It is worth noting that there is no response during the Cerenkov resonance for the electromagnetic wave (EMW), as the Cerenkov effect primarily pertains to electrostatic waves. The ADE mechanism from classical theory is analysed in appendix.

IV. CRITICAL TRAPPING THRESHOLD OF ADE

We found that the ADE is equivalent to an effective damping force, hindering the electron acceleration process. Therefore, if the intensity of the electromagnetic wave is increased, it is theoretically possible to achieve a balance with the electrostatic field force, causing the electron to no longer be accelerated by the electrostatic field. Next, we will demonstrate the existence of this equilibrium by varying the electromagnetic wave field intensity.

Let us consider an EMW with only left-hand polarized circular wave, where the wave-vector k and frequency ω of the EMW are set as $k = 10^5/\text{m}$ and $\omega = 1.5 \omega_0$. Here $\omega_0 = (eB_0)/m_e$ and k is parallel to the static magnetic field. The electrostatic field and the static magnetic field are set as $E_0 = -2.5 \text{ V}$ and $B_0 = 2 \times 10^{-2} \text{ T}$ respectively. As shown in Fig. 7, when we increase the energy of EMW, the parallel velocity will be trapped in the resonant condition and stops increasing while the perpendicular velocity increase continuously when the ratio E_w/E_0 exceeds a certain threshold. The trapped electron's orbit and moment are shown in Fig. 8.

The threshold field E can be obtained by modifying the EMW intensity using a dichotomy control approach based on the final parallel velocity with a long enough time. The critical ratios of E_c/E_0 with dimensionless parameters $\frac{\omega^2}{kc\omega_0}$ are

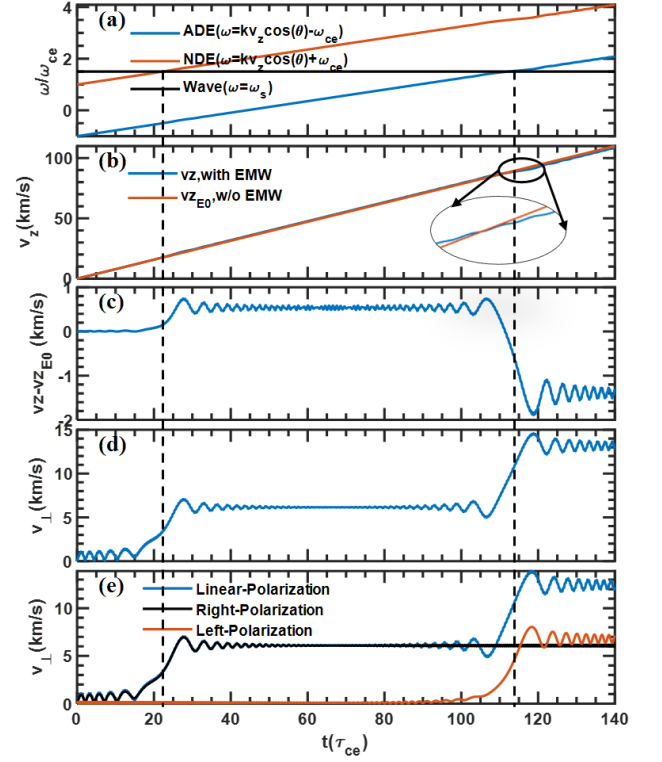


FIG. 6. Kinetic evolution of electron in magnetic field with EMW during acceleration. (a) Wave frequencies of anomalous Doppler frequency, normal Doppler frequency and source wave frequency. (b) Translational velocity v_z with and without EMW (c) The change of parallel velocity caused by EMW. (d) Cyclotron velocity v_\perp . (e) Interaction with Linear, Right-hand circular, Left-hand circular polarization.

shown in Fig. 9 (here the angles between B_0 and wavevector k are $\theta = 0, 15^\circ, 30^\circ$). As observed, a larger angle between k and B_0 results in a less critical ratio for trapping electrons. This possibility could be attributed to the increase in the electric field along the parallel direction as the angle increases, which leads to an increase in the halting force along that direction. It is apparent that with only small intensity of left-hand circular polarized wave we can halt the increase of the electron's parallel momentum and transfer energy from electrostatic field to rotational energy by ADE. For example, in Tokamak the toroidal electric field is about 0.2 V/m , the threshold electric field for left-hand circular polarized wave to trap electron is about $E_p = 2 \text{ V/m}$ in the plasma (the corresponding energy flux is about 0.04 W/m^2 for $k = 2 \times 10^3/\text{m}$ and $\omega = \omega_{ce}$ with $B_0 = 2 \text{ T}$).

V. SIMULATION WITH TOKAMAK PARAMETERS

In order to check the validity in high magnetic fields and the angle dependence of ADE, we choose uniform field of $B = 2 \text{ T}$ and $E_0 = -0.2 \text{ V/m}$, which are typical parameters

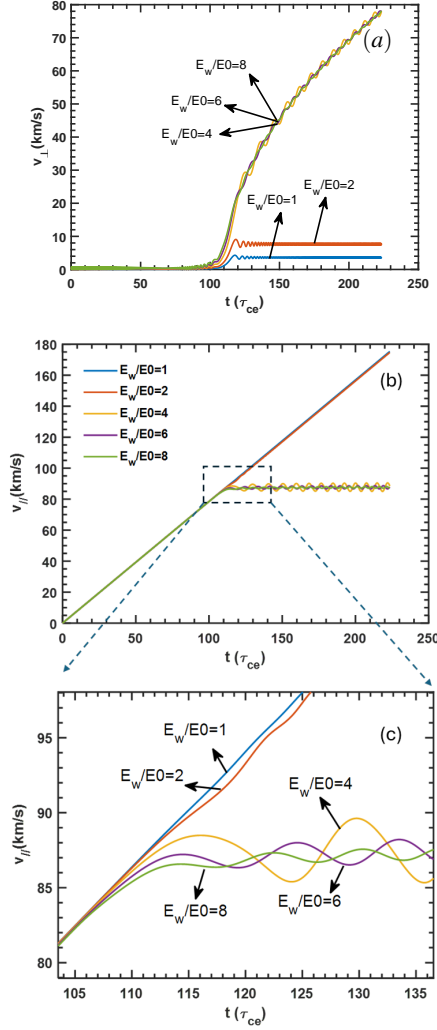


FIG. 7. Time trace of velocity under different ratio of E_p/E_0 . (a) vertical velocity (b) parallel velocity (c) Zoom in parallel velocity.

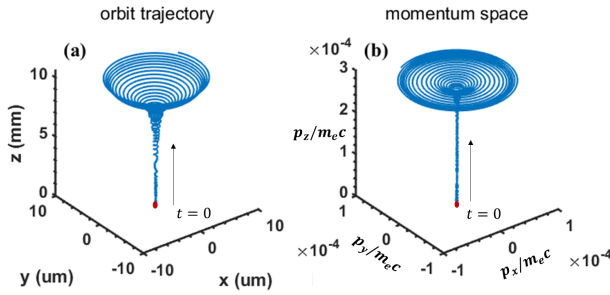


FIG. 8. The trapped electrons orbit and momentum

of a Tokamak during startup⁹. For a plane left-hand circularly polarized wave, $f = 56$ GHz, $E_p = 40$ V/m, and $k = 2.6 \times 10^3$ /m, the energy flux of the wave is about 9 W/m^2 . Using the powerful parallelism of supercomputer, We can simultaneously calculate the interaction of 500 electrons with a left-handed circularly polarized wave at 500

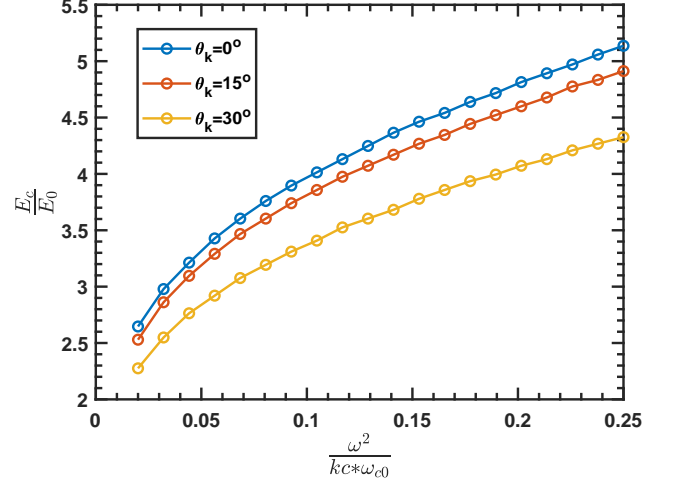


FIG. 9. Critical ratio of E_c/E_0 with normalized parameter $\frac{\omega^2}{kc\omega_0}$, where $E_0 = -2.5 \text{ V}$, $B_0 = 2 \times 10^{-2} \text{ T}$, $\omega = 1.5\omega_0$ and the refractive index ranges from 4 to 50.

different incident angles θ in the range of 0 to 90 degrees, demonstrating the dependence of the ADE effect on the angle. The time step in the simulation is set at $\Delta t = 1 \times 10^{-14} \text{ s}$ to ensure the convergence of the results. The results are shown in Fig. 10, where the dashed yellow line represents the earliest resonant time that satisfies the relation $\omega - \vec{k} \cdot \vec{v} + \omega_{ce} = 0$. It is evident that as the angle θ increases, the onset of resonance is delayed, and the requisite speed for resonance is heightened. Following the initiation of resonance, the rotational velocity v_{\perp} witnesses a swift augment, whilst the parallel velocity gets ensnared within the resonant region, thereby ceasing any further increment. These results indicate that even with a small energy of left-hand polarized waves, we can suppress runaway electrons and transfer the acceleration from the electrostatic field to rotational energy in Tokamak parameters.

VI. EMW DRIVES ADE IN MAGNETIZED PLASMA

Runaway electrons present a significant threat to tokamak devices due to their potential to damage plasma-facing components (PFCs)³⁵ through high-energy impacts. Harnessing the ADE effect in tokamaks offers a promising approach to controlling runaway energy, provided three critical conditions are satisfied:

1. The existence of a left-hand polarized wave component when electrons move in the direction of the magnetic field;
2. The phase velocity of the electromagnetic wave must remain below the speed of light in a vacuum.
3. The wave must possess sufficient energy to counteract the accelerating velocity of the electrons. Meeting these conditions enables the establishment of controllable resonant interactions essential for mitigating runaway electrons.

Consider waves in cold magnetized plasmas where

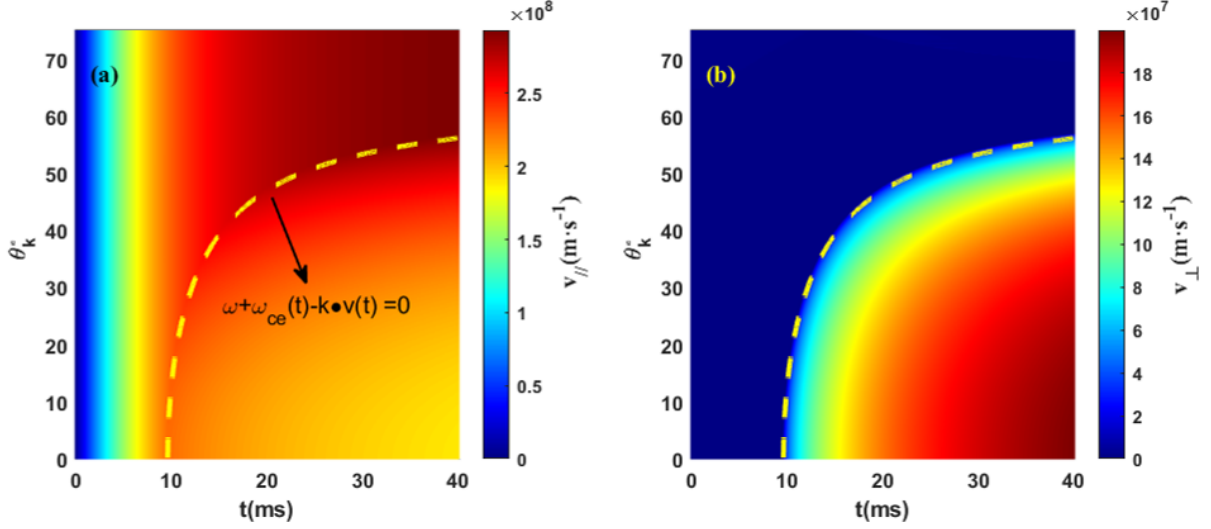


FIG. 10. Time evolution of v_{\perp} and v_{\parallel} by emw with different incident angle θ_k^o

$\omega_{pe}/\omega_{ce} = 0.5$, from Appleton-Hartree formula (It is commonly believed that the cold plasma dispersion is generally adequate for calculating wave propagation when the phase velocity significantly exceeds the thermal velocity of electrons in the plasma.):

$$\begin{aligned}
 & \omega^{10} - \omega^8 (2k^2 c^2 + \omega_{ce}^2 + \omega_{ci}^2 + 3\omega_{pe}^2) \\
 & + \omega^6 \left[k^4 c^4 + (2k^2 c^2 + \omega_{pe}^2) (\omega_{ci}^2 + \omega_{pe}^2) + (\omega_{pe}^2 + \omega_{ce} \omega_{ci})^2 \right] \\
 & - \omega^4 \left[k^4 c^4 (\omega_{ce}^2 + \omega_{ci}^2 + \omega_{pe}^2) + 2k^2 c^2 (\omega_{pe}^4 + \omega_{ce} \omega_{ci})^2 \right. \\
 & + k^2 c^2 \omega_{pe}^2 (\omega_{ce}^2 + \omega_{ci}^2 - \omega_{ce} \omega_{ci}) (1 + \cos^2 \theta) \\
 & + \omega_{pe}^2 (\omega_{pe}^2 + \omega_{ce} \omega_{ci})^2 \left. \right] + \omega^2 \left[k^4 c^4 \omega_{pe}^2 \cos^2 \theta \right. \\
 & + k^2 c^2 \omega_{pe} \omega_{ce} \omega_{ci} (\omega_{pe} + \omega_{ce} \omega_{ci}) (1 + \cos^2 \theta) \left. \right] \\
 & - k^4 c^4 \omega_{ce}^2 \omega_{ci}^2 \omega_{pe}^2 \cos^2 \theta = 0
 \end{aligned} \tag{19}$$

Where ω is the wave frequency and k represents the wavevector. The ω and k are both depend on the electron cyclotron frequency (ω_{ce}), the plasma frequency (ω_{pe}) and the ion cyclotron frequency (ω_{ci}). Here θ is the angle between \vec{k} and static magnetic field \vec{B} . The dispersion relationship can be illustrated in Fig. 11(a), where the blue color represents the wavevector $\theta = 0$, while the red color represents $\theta = \frac{\pi}{2}$. As shown in Fig. 11(c), the black line refers to the wave in the vacuum. Only waves in low frequency region and high frequency region shown in Fig. 11(d) have the ability to cause ADE, where the phase velocity $v_p = \frac{\omega}{k} < c$ in these regions. The polarization vector of the wave can be expressed as³⁶

$$(e_x, e_y, e_z) = \left(1, i \frac{\frac{\omega_{pe}^2 \omega_{ce}}{\omega}}{\omega^2 - k^2 c^2 - \omega_{ce}^2 - \omega_{pe}^2 + \frac{k^2 c^2 \omega_{ce}^2}{\omega^2}}, \frac{k_{\parallel} k_{\perp} c^2}{\omega_{pe}^2 + k_{\perp}^2 c^2 - \omega_{ce}^2} \right) \tag{20}$$

The electric field of the wave can be written as $\vec{E} = E_0 (e_x + e_y + e_z) \exp(i(kr - \omega t))$. When the imaginary part

of e_y is positive, the main component of the wave is a right-hand polarized wave. Otherwise, it is predominantly left-hand polarized wave. The black dashed line represents the boundary between two different types of waves where $e_y = \infty$. Between the pair of dashed lines, the wave predominantly exhibits left-hand polarization. Conversely, beyond these demarcated lines, the wave is mainly right hand polarized. As depicted in Fig. 11(b), low frequency region comprises whistlers and magnetized electron plasma wave, where all electromagnetic waves mainly exhibit right-hand polarization. Conversely, in high frequency region, Extraordinary waves display left-hand polarization when θ is in close proximity to $\pi/2$.

Consider the resonant condition

$$\omega + n\omega_{ce} - \vec{k} \cdot \vec{v} = 0 \tag{21}$$

When the runaway electron's moment match the resonant condition, it is possible to stimulate the intrinsic waves in plasma. Here we choose $n = 1$ for ADE, and $n = 0$ for Landau resonant. The term $n = -1$ is disregarded in this context since NDE is not important in high frequency region due to its requires right-hand polarized wave. By combining Eq. (19) and Eq. (21), we establish the relationship between the wave and resonance moment, as illustrated in Fig. 12. In high frequency region, for ADE, resonance curves with dimensionless resonance momentum greater than 1 are converged to right bottom region shown in Fig. 12(c), which corresponds to the Extraordinary wave with frequency range $(\omega_{ce}, \sqrt{\omega_{ce}^2 + \omega_{pe}^2})$. This explains why Extraordinary

wave near the frequencies of $(\omega_{ce}, \sqrt{\omega_{ce}^2 + \omega_{pe}^2})$ are excited when electron scattering occurs in magnetized devices^{14,19}. Furthermore, the dimensionless Landau resonant momentum for most of low frequency region is greater than 1, as shown in Fig. 12(a). This suggests less attenuation of waves by background thermal electrons and makes wave

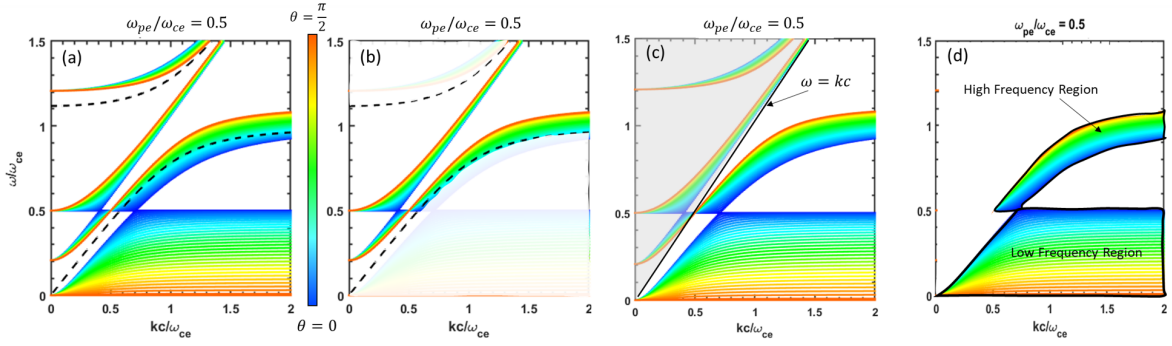


FIG. 11. Dispersion relationship in cold magnetized plasma. (a) Complete dispersion relationship in cold magnetized plasma. (b) Region dominated by left-hand polarization. (c) Region where phase velocity is smaller than the speed of light in vacuum. (d) High-frequency and low-frequency regions.

formation in the low frequency region easier. For the high frequency region, When the energy of high-energy runaway electrons exceeds 10 MeV (reduced momentum $p > 20$), the resonance curves of electromagnetic waves excited by the ADE effect almost always pass through left top region depicted in Fig. 12(d). This region corresponds closely to the whistler waves zone where whistler waves propagate parallel to the magnetic field. Therefore, in Tokamak experiments, the observation of whistler waves is typically associated with the detection of high energy electrons with energy exceeding 10 MeV³⁷. The dimensionless Landau resonance momentum for low frequency region is less than 1, as depicted in Fig. 12(b). This indicates a higher degree of wave attenuation by background thermal electrons compared to high frequency region, making wave formation in region B more challenging.

Based on the above discussion, electromagnetic waves in the high frequency region are more prone to exciting Anomalous Doppler Resonance due to polarization and damping, while waves in the low frequency region are better suited for heating background electrons through Landau resonant, such as low-hybrid wave heating. Experiments show that runaway electrons can stimulate extraordinary waves with frequencies in the range ω_{ce} to ω_{uh} through ADE and transport their parallel energy to rotational energy^{14,38}. It is natural to consider utilizing the reverse process by injecting extraordinary waves to suppress runaway electrons.

VII. INJECT EXTRAORDINARY WAVE TO SUPPRESS THE RUNAWAY ELECTRONS

The characteristic frequency with $\vec{k} \perp \vec{B}$ in Tokamak plasma is shown in Fig. 13 under condition where the intensity on the axis toroidal B is $B_0 = 2$ T, $n_{e0} = 1 \times 10^{19}/\text{m}^3$ and the density along the minor radius has profile as $n_e = n_{e0}(1 - r^2)$, r is the normalized minor radius. The X-Wave will slow down near upper-hybrid frequency layer and reflect at right cut-off frequency layer. Therefore, it is necessary to input extraordinary wave from high field side of Tokamak, whereas it will be reflected at the right cut-off frequency layer when input from the lower-field side. Different frequency

corresponds to different position. We can adjust the frequency of the extraordinary wave to align with the region where runaway events are more likely to occur (such as in the core of Tokamak). Since the power requirement for trapping runaway electrons is not higher than KW, it is worth noting that precise frequency adjustments to match the core of the Tokamak based on real-time plasma density diagnosis is possible to achieve.

VIII. SUMMARY

This study presents a simulation of the interaction between electrons and plane EMW within uniform magnetic and electrostatic field. The simulation demonstrates that the parallel velocity of electrons can be rapidly converted into rotational velocity during the ADE, with only left-hand circular polarization waves contributing to the ADE. When the electric field surpasses the critical field, the EMW can capture the parallel momentum of electrons and perpetually transfer energy from the parallel electrostatic field to rotational energy and resonance waves. The proportion between the loss of parallel energy and the augmentation in rotational energy aligns with both quantum theory and the simulation results. Furthermore, this study also delves into the fundamental physics of ADE from the basic energy-moment-angular moment conservation. We ascertain that the extraordinary wave, situated near the upper-hybrid resonance, emerges as the most apt candidate wave for mitigating runaway electrons. By injecting the extraordinary wave from the high-field side of the Tokamak, we can potentially inhibit the runaway electrons at the Tokamak core. It is possible to suppress runaway electrons at the core of the Tokamak based on real-time plasma density diagnosis by dynamically adjusting wave frequencies, where the field intensity needed to achieve this suppression is only a few orders of magnitude greater than the electrostatic field E_0 .

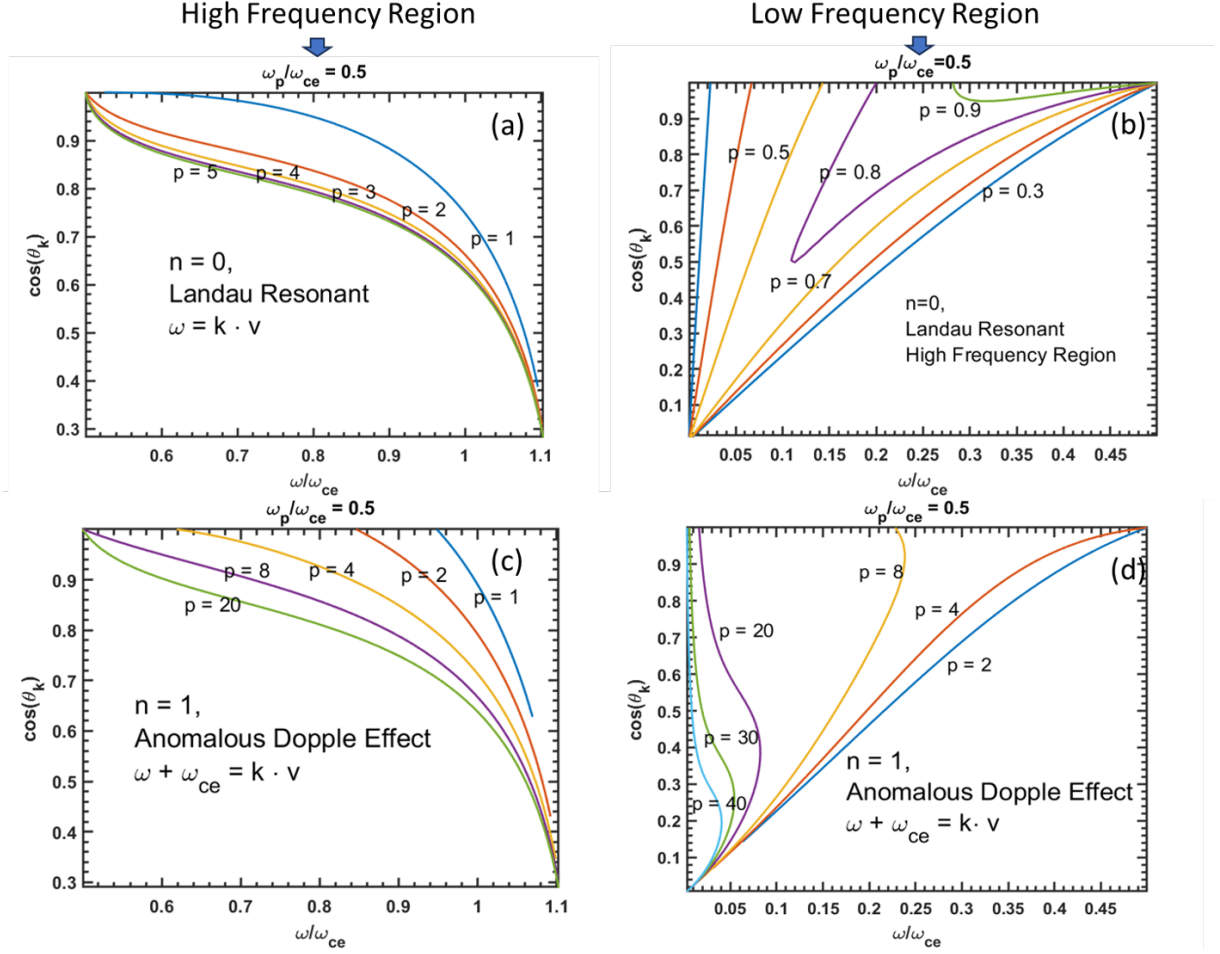


FIG. 12. In high frequency region, the lower left boundary corresponds to the up-hybridized resonance frequency for different angles. In low frequency region, the lower right boundary corresponds to the low-hybridized resonance frequency for different angles. (a) (b) dimensionless moment of Landau resonance in high frequency region and B. (c) (d) dimensionless moment of ADE in high frequency low frequency region

ACKNOWLEDGMENTS

This work is supported by National Magnetic Confinement Fusion Energy Program of China under Contract No. 2019YFE03020001, Collaborative Innovation Program of Hefei Science Center, CAS under Contract No. 2021HSC-CIP010 and the Fundamental Research Funds for the Central Universities.

IX. APPENDICES

Further investigation is necessary to comprehend why left-handed circular polarization is responsible for the ADE and what causes the scattering of the electron's parallel momentum to rotational moment. In this Appendixes, our objective is to understand this phenomenon using classical electrodynamic theory.

A. EMW polarization

During the resonance with the induced wave, the rotation of the electromagnetic field and electron motion become synchronized. The wave frequency is equal to the electron cyclotron frequency in the frame of a gyro-center moving electron. The frequency and wavevector in the two frames, namely the laboratory frame and the moving gyro-center electron frame, can be directly linked through the Lorentz transformation¹⁰:

$$\begin{bmatrix} \vec{k} \\ \frac{\omega}{c} \end{bmatrix} = \begin{bmatrix} \vec{\alpha} & +\gamma\vec{\beta} \\ +\gamma\vec{\beta} & \gamma \end{bmatrix} \begin{bmatrix} \vec{k}' \\ \frac{\omega'}{c} \end{bmatrix} \quad (22)$$

where $\vec{k} = k_x\vec{e}_x + k_y\vec{e}_y + k_z\vec{e}_z$ ($\vec{k}' = k'_x\vec{e}_x + k'_y\vec{e}_y + k'_z\vec{e}_z$) and ω ($\omega' = \omega_0$) are wavevector and the frequency in the laboratory frame (the moving gyro-center electron frame) respectively. $\vec{v} = v\vec{e}_z$ is the parallel velocity of the electron with normalized form being $\vec{\beta} = \frac{\vec{v}}{c}$, $\gamma = (1 - \beta^2)^{-\frac{1}{2}}$ is the Lorentz factor. $\vec{\alpha} = \mathbf{I} + (\gamma - 1)\frac{\vec{\beta}\vec{\beta}}{\beta^2}$ where \mathbf{I} is unit tensor. From

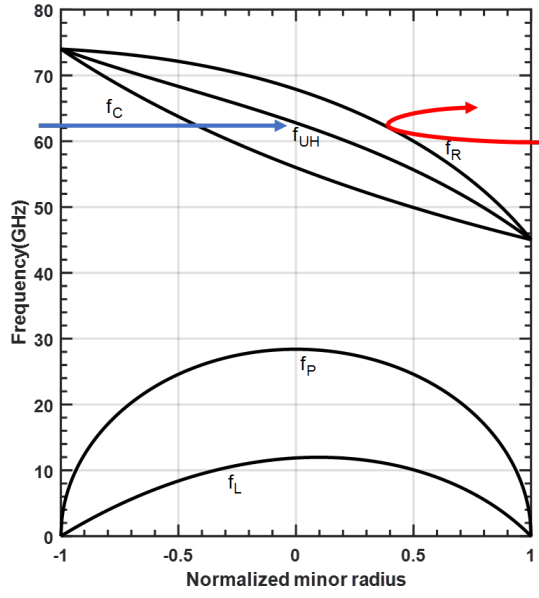


FIG. 13. Characteristic frequency distribution in plasma. f_c is electron cyclotron frequency, f_{UH} is upper hybrid frequency, f_P is plasma frequency and f_L is left-handed cutoff frequency, f_R is Right-handed cutoff frequency.

relationship (13),

$$\omega = \gamma\omega_0 + \gamma v k'_z \quad (23)$$

$$k_z = \gamma k'_z + \gamma \frac{v}{c} \frac{\omega_0}{c} \quad (24)$$

Substitute k_z with $\frac{\omega}{c} \cos(\theta)$ and combine with (14)(15), we get the frequency in laboratory frame

$$\omega = \frac{\omega_{ce}}{1 - \frac{v}{c} \cos(\theta)} \quad (25)$$

where ω_{ce} representing the right-hand rotation for an electron in magnetic field. In the case of the NDE, it is essential to note that the resonant velocity, denoted as v_{NDE}/c' , must satisfy the condition $v_{NDE}/c' < 1$. This condition ensures that both angular frequencies, ω and ω_{ce} (where $\omega_{ce} = \frac{\omega_0}{\gamma}$), share the same sign. Consequently, it proves only waves exhibiting right-hand polarization can induce the NDE. In the case of the ADE, a different scenario arises. The resonant velocity is expressed as $v_{ADE} = \frac{\omega + \omega_{ce}}{k_z}$. For ADE to occur, the condition $\frac{v_{ADE}}{c'} \cos(\theta) = 1 + \left| \frac{\omega_{ce}}{\omega} \right| > 1$ must be satisfied. Consequently, it is evident that ω and ω_{ce} have opposite signs in Eq.(25), indicating that only left hand circular polarization waves are responsible for inducing the ADE. This feature has been rarely considered in previous theories of ADE. It is worth noting that the requirement of left-hand circular polarization for ADE performs does not mean that the wave should be completely left-hand circularly polarized. As long as there exists a component of left-hand circular polarization in the direction of the cyclotron electron's motion, it is possible to trigger the ADE, as observed with whistle waves in Tokamak systems²⁰.

B. Scattering

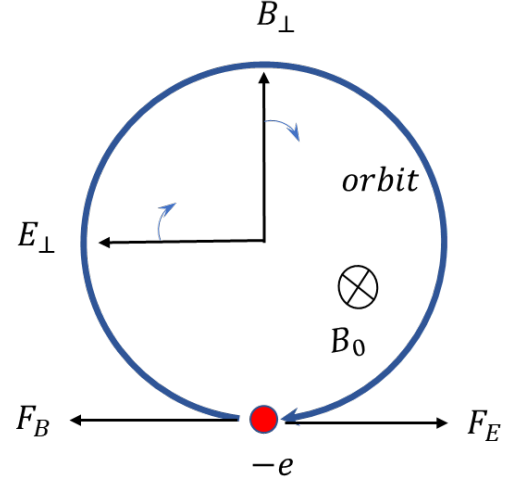


FIG. 14. Scheme of electron movement in uniform magnetic field with EMW, here B_0 is static magnetic field, E_\perp and B_\perp are refer to electric field and magnetic field of EMW respectively. F_B represents magnetic force of EMW, F_E represents electric force of EMW

The scattering results shown in Fig. 6 can be interpreted from classical electrodynamics as follows: Considering the circular polarization of EMW has the same frequency as ω_0 during resonance in the moving gyro-center electron frame, as shown in Fig. 14, where the wavevector k parallel to the z -axis, the perpendicular forces exerted by the magnetic field ((B)) and electric field ((E)) of EMW can be described as follows:

$$\vec{F}_{B\perp} = (-e) \vec{v}_\parallel \times \vec{B}_\perp = \frac{ev_\parallel k_z}{\omega} \vec{E}_\perp \quad (26)$$

$$\vec{F}_{E\perp} = (-e) \vec{E}_\perp \quad (27)$$

the forces $\vec{F}_{B\perp}$ and $\vec{F}_{E\perp}$ have opposite directions. The net force on electron in perpendicular direction is

$$\vec{F}_\perp = \vec{F}_{B\perp} + \vec{F}_{E\perp} = e\vec{E}_\perp \left(\frac{v_\parallel}{c'} - 1 \right) = \vec{F}_{E\perp} \left(1 - \frac{v_\parallel}{c'} \right) \quad (28)$$

where $c' = \omega/k$, $k_z = k$. The electron velocity v_\perp has tendency to parallel to \vec{F}_\perp by changing the rotation phase of electron during resonant with EMW, as shown in Fig. 14. The force from EMW paralleled to z is:

$$\vec{F}_\parallel = -e \left(\vec{v}_\perp \times \vec{B}_\perp \right) = \frac{-e \vec{v}_\perp \cdot \vec{E}_\perp}{c'} = \frac{\vec{v}_\perp \cdot \vec{F}_{E\perp}}{c'} \quad (29)$$

the total work by EMW is

$$P = \vec{F}_\parallel \cdot \vec{v}_\parallel + \vec{F}_\perp \cdot \vec{v}_\perp = \vec{v}_\perp \cdot \vec{F}_{E\perp} \quad (30)$$

For NDE, $\frac{v_\parallel}{c'} < 1$, $|\vec{F}_{B\perp}| < |\vec{F}_{E\perp}|$, the rotational velocity v_\perp tend to parallel to $\vec{F}_{E\perp}$ under external EMW, then $\vec{v}_\perp \cdot \vec{F}_{E\perp} > 0$, $\vec{F}_\parallel \cdot \vec{v}_\parallel < 0$, $\vec{F}_\perp \cdot \vec{v}_\perp > 0$, $P > 0$, EMW will heat and

exert a parallel force, causing the electron to accelerate along the z-axis.

For the Cerenkov Effect(CE), where $\frac{v_{\parallel}}{c} = 1$ and $\vec{F}_{\perp} = 0$, the absence of a vertical force from EMW results in a random phase angle between \vec{v}_{\perp} and $\vec{F}_{E\perp}$, so the average of $\langle \vec{F}_{\parallel} \rangle = 0$, $\langle \vec{F}_{\perp} \cdot \vec{v}_{\perp} \rangle = 0$, which means that the EMW doesn't take part in Cerenkov effect. The longitudinal wave is more relevant to Cerenkov resonant, which also known as Landau resonant, where the electron rides on the crest of the wave, being exposed to a force thus continually absorbs energy from the wave until its velocity increases and drops out of phase with the wave. such as lower hybrid waves in plasma¹⁵.

For ADE, $\frac{v_{\parallel}}{c} > 1$, $|\vec{F}_{B\perp}| > |\vec{F}_{E\perp}|$, the rotational velocity v_{\perp} tend to parallel to $\vec{F}_{B\perp}$ under external EMW, then $\vec{v}_{\perp} \cdot \vec{F}_{E\perp} < 0$, $\vec{F}_{\parallel} < 0$, $\vec{F}_{\parallel} \cdot \vec{v}_{\parallel} < 0$, $\vec{F}_{\perp} \cdot \vec{v}_{\perp} > 0$, $P < 0$. As a result, the electron will convert its kinetic energy into rotational energy and emit EMW. It is interesting to note that the magnetic field of the EMW performs positive work on the electron in the perpendicular direction and negative work in the parallel direction. The behavior of magnetic field in the EMW acts like a bridge connecting the parallel and perpendicular directions, transferring energy from kinetic energy to rotational internal energy. This fundamental physics process helps us understand why parallel kinetic energy can be converted into rotational energy.

C. Consistency between quantum theory and simulation

This section focuses on analyzing the energy flow during the Anomalous Doppler Resonance of electron excited by a left-hand circularly polarized wave with wave vector k parallel to the magnetic field B_0 . In the vertical direction, the electron is only subjected to work by the electromagnetic wave, which can be divided into two components: $W_{B\perp}$, representing the work done by the magnetic field of the electromagnetic wave, and $W_{E\perp}$, representing the work done by the electric field of the electromagnetic wave. Here, $W_{B\perp} = \int \vec{F}_{B\perp} \cdot \vec{v}_{\perp} dt$ and $W_{E\perp} = \int \vec{F}_{E\perp} \cdot \vec{v}_{\perp} dt$. The total work of the EMW in the vertical direction is $W_{\perp emw} = W_{B\perp} + W_{E\perp}$. In the parallel direction, both the electrostatic field and the electromagnetic wave can exert work on the electron. This includes W_{E0} , representing the work done by the electrostatic field, and $W_{\parallel emw}$, representing the work done by the electromagnetic wave. Specifically, $W_{E0} = \int \vec{F}_{E0} \cdot \vec{v}_{\parallel} dt$ and $W_{\parallel emw} = \int \vec{F}_{\parallel} \cdot \vec{v}_{\parallel} dt$, where \vec{F}_{\parallel} is Eq.(29). The total work in the parallel direction is given by $W_{\parallel} = W_{E0} + W_{\parallel emw}$. All this work can be calculated numerically. Here, we use the same setup as above with $E_c/E_0 = 6$, where the electron can be trapped by the EMW. Numerical results are shown in Fig. 15, where $T_{k\perp}$ and $T_{k\parallel}$ are rotational energy and parallel kinetic energy of electron respectively. Fig. 15(a) shows that EMW performs negative work on the electron in the parallel direction while positive work in the vertical direction, the total work of EMW on electron is negative, which means the electron transfers energy to EMW. In the parallel direction, as shown in Fig. 15(b), the electromagnetic wave performs negative work,

which is balanced by the positive work from the electrostatic field. This equilibrium causes the electrons velocity to stop increasing. In the vertical direction (Fig. 15(c)), the magnetic field of the EMW performs positive work, while the electric field of the EMW performs negative work. The total work in the vertical direction done by the EMW is equal to the change in kinetic energy of the electron, denoted as $T_{k\perp}$. This observation aligns well with the previous analysis (IX B).

Let's consider the energy transformation coefficient. The decreases energy of the electron in the parallel direction is $\Delta T_{k\parallel} = -W_{\parallel emw}$, while the increase energy of the electron in the vertical direction is $\Delta T_{k\perp} = W_{\perp emw}$, the increased energy of EMW is $W_{emw} = -(W_{\parallel emw} + W_{\perp emw})$. The ratio of the loss of parallel energy of the electron to the vertical energy is represented by $\eta_p = \frac{\Delta T_{k\perp}}{\Delta T_{k\parallel}}$, while to EMW is $\eta_w = \frac{W_{emw}}{\Delta T_{k\parallel}}$. The numerical results of η_p and η_w are depicted in Fig. 15(d) and . According to quantum theory, the decreases energy of the electron in the parallel direction is $\Delta T = \Delta \vec{p} \cdot \vec{v} = \hbar k v \cos \theta$. The increase in rotational energy is $\Delta U = n \hbar \omega_{ce}$, where we choose $n = 1$ for the anomalous Doppler effect at here, the photon energy is $\hbar \omega$. According to the simulation setup with the following parameters: $k = 10^5/m$, $\omega = -1.5\omega_0$, $\theta = 0$, and $B = 0.02, T$, the resonant velocity is approximately $v = 86.8, km/s$. Consequently, the ratio of $\eta_p = \frac{\Delta U}{\Delta T} = \frac{\omega_{ce}}{kv} = 0.4$, and the ratio of $\eta_w = \frac{\omega}{kv} = 0.6$. These values align well with classical electrodynamics calculations as shown in Fig. 15(d).

- ¹M. Rosenbluth and S. Putvinski, "Theory for avalanche of runaway electrons in tokamaks," Nuclear fusion **37**, 1355 (1997).
- ²J. Liu, Y. Wang, and H. Qin, "Collisionless pitch-angle scattering of runaway electrons," Nuclear Fusion **56**, 064002 (2016).
- ³V. L. Ginzburg, "Certain theoretical aspects of radiation due to superluminal motion in a medium," Soviet Physics Uspekhi **2**, 874–893 (1960).
- ⁴Y. N. Wei, W. Yan, Z. Y. Chen, R. H. Tong, Z. H. Jiang, and Z. J. Yang, "Runaway current suppression by secondary massive gas injection during the disruption mitigation phase on j-text," Plasma Physics and Controlled Fusion **61** (2019), 10.1088/1361-6587/ab210b.
- ⁵L. Zeng, Z. Y. Chen, Y. B. Dong, H. R. Koslowski, Y. Liang, Y. P. Zhang, H. D. Zhuang, D. W. Huang, and X. Gao, "Runaway electron generation during disruptions in the j-text tokamak," Nuclear Fusion **57** (2017), 10.1088/1741-4326/aa57d9.
- ⁶I. Frank, "Optics of light sources moving in refractive media: Vavilov-cherenkov radiation, though interesting, is but an experimental instance of a more general problem," Science **131**, 702–712 (1960).
- ⁷M. V. Nezlin, "Negative-energy waves and the anomalous doppler effect," Soviet Physics Uspekhi **19**, 946 (1976).
- ⁸L. V. Filatov and V. F. Melnikov, "The role of the anomalous doppler effect in the interaction of energetic electrons with whistler turbulence in flare loops," Geomagnetism and Aeronomy **61**, 1183–1188.
- ⁹C. Liu, E. Hirvijoki, G. Y. Fu, D. P. Brennan, A. Bhattacharjee, and C. Paz-Soldan, "Role of kinetic instability in runaway-electron avalanches and elevated critical electric fields," Physical Review Letters **120** (2018).
- ¹⁰X. H. Shi, X. Lin, I. Kaminer, F. Gao, Z. J. Yang, J. D. Joannopoulos, M. Soljacic, and B. L. Zhang, "Superlight inverse doppler effect," Nature Physics **14** (2018).
- ¹¹H. W. Lu, L. Q. Hu, Y. D. Li, G. Q. Zhong, S. Y. Lin, P. Xu, and E. Team, "Investigation of fast pitch angle scattering of runaway electrons in the east tokamak," Chinese Physics B **19** (2010).
- ¹²D. Campbell, A. Eberhagen, and S. J. N. f. Kissel, "Analysis of electron cyclotron emission from non-thermal discharges in asdex tokamak," Nucl. Fusion **24**, 297 (1984).
- ¹³D. Boyd, F. Stauffer, and A. J. P. R. L. Trivelpiece, "Synchrotron radiation from the atc tokamak plasma," **37**, 98 (1976).
- ¹⁴S. J. Freethy, K. G. McClements, S. C. Chapman, R. O. Dendy, W. N. Lai, S. J. P. Pamela, V. F. Shevchenko, and R. G. L. Vann, "Electron kinetics

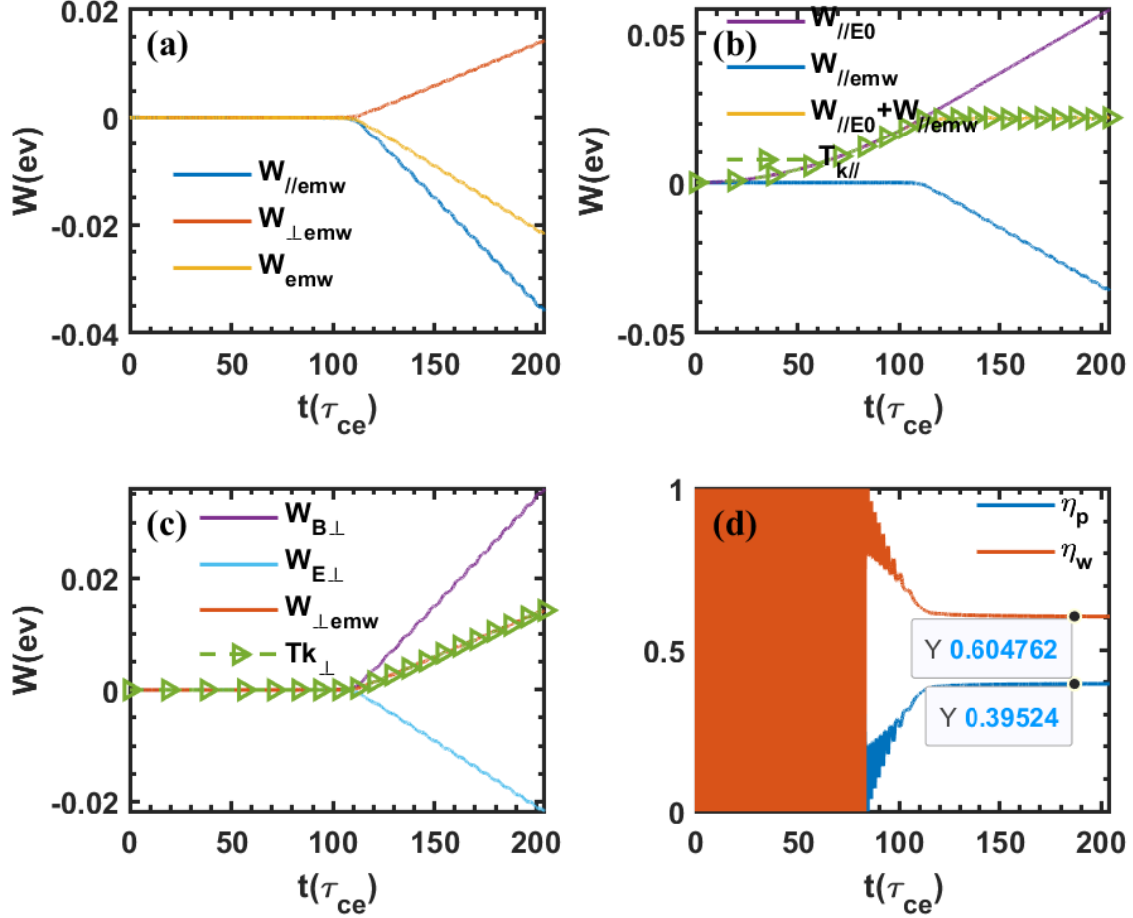


FIG. 15. Energy analysis of EMW and electrostatic on the resonant electron during ADR(Anomalous Doppler Resonance). (a) EMW's energy analysis for both direction (b) parallel direction. (c)vertical direction (d) conversion ratio of electrostatic work to EMW (η_w) and to internal energy of electron (η_p)

- inferred from observations of microwave bursts during edge localized modes in the mega-amp spherical tokamak," *Physical Review Letters* **114** (2015).
- ¹⁵F. Santini, E. Barbato, F. Demarco, S. Podda, and A. Tuccillo, "Anomalous doppler resonance of relativistic electrons with lower hybrid waves launched in the frascati tokamak," *Physical Review Letters* **52**, 1300–1303 (1984).
- ¹⁶Z. Chen, J. Zhu, H. Ju, Q. Du, Y. Shi, H. Liang, M. Li, and W. Cai, "Characteristics of the runaway electron beam instability in the ht-7 tokamak," *Journal of plasma physics* **75**, 661–667 (2009).
- ¹⁷W. Bin, C. Castaldo, F. Napoli, P. Buratti, A. Cardinali, A. Selce, and O. Tudisco, "First intrashot observation of runaway-electron-driven instabilities at the lower-hybrid frequency range under iter-relevant plasma-wave dispersion conditions," *Physical Review Letters* **129** (2022).
- ¹⁸B. Kadomtsev and O. Pogutse, "Electric conductivity of a plasma in a strong magnetic field," *Sov. Phys. JETP* **26**, 1146 (1968).
- ¹⁹E. Shustin, P. POPOVICH, and I. Kharchenko, "Transformation of electron beam distribution function following cyclotron interaction with a plasma," *SOVIET PHYSICS JETP* **32** (1971).
- ²⁰D. A. Spong, W. Heidbrink, C. Paz-Soldan, X. Du, K. Thome, M. Van Zeeland, C. Collins, A. Lvovskiy, R. Moyer, and M. Austin, "First direct observation of runaway-electron-driven whistler waves in tokamaks," *Physical Review Letters* **120**, 155002 (2018).
- ²¹N. Ginzburg, "Nonlinear theory of electromagnetic wave generation and amplification based on the anomalous doppler effect," *Radiophysics and Quantum Electronics* **22**, 323–330 (1979).
- ²²L. B. Kong, Z. L. Hou, and C. R. Xie, "The self-consistent nonlinear theory of electron cyclotron maser based on anomalous doppler effect," *Applied Physics Letters* **98** (2011).
- ²³V. L. Ginzburg, "Radiation of uniformly moving sources (vavilov-cherenkov effect, transition radiation, and other phenomena)," *PHYSICS USPEKHI C/C OF USPEKHI FIZICHESKIKH NAUK* **39**, 973–982 (1996).
- ²⁴T. H. Kho and A. T. Lin, "Slow-wave electron-cyclotron maser," *Physical Review A* **38**, 2883–2888 (1988).
- ²⁵V. L. Ginzburg, "Vavilov-cherenkov effect and anomalous doppler effect in medium which wave phase velocity exceeds velocity of light in vacuum," *Zhurnal Eksperimentalnoi I Teoreticheskoi Fiziki* **62**, 173 (1972).
- ²⁶J. Benford, J. A. Swegle, and E. Schamiloglu, *High power microwaves* (CRC press, 2007).
- ²⁷R. L. Zhang, J. Liu, H. Qin, Y. L. Wang, Y. He, and Y. J. Sun, "Volume-preserving algorithm for secular relativistic dynamics of charged particles," *Physics of Plasmas* **22** (2015).
- ²⁸I. E. Tamm, "General characteristics of radiation emitted by systems moving with superlight velocities with some applications to plasma physics," *Nobel Lectures* **18**, 122–133 (1959).

- ²⁹I. Frank, "Optics of light sources moving in refractive media: Vavilov-cherenkov radiation, though interesting, is but an experimental instance of a more general problem," *Science* **131**, 702–712 (1960).
- ³⁰Y. Wang, J. Liu, H. Qin, Z. Yu, and Y. Yao, "The accurate particle tracer code," *Computer Physics Communications* **220**, 212–229 (2017).
- ³¹Y. Wang, H. Qin, and J. Liu, "Multi-scale full-orbit analysis on phase-space behavior of runaway electrons in tokamak fields with synchrotron radiation," *Physics of Plasmas* **23** (2016).
- ³²V. V. Alikeev and V. V. Parail, "Current drive by electron-cyclotron waves," *Plasma Physics and Controlled Fusion* **33**, 1639–1656 (1991).
- ³³M. A. LIEBERUN, "Theory of electron cyclotron resonance heating. ii. long time and stochastic effects," *Plasma Physics* (1972).
- ³⁴N. Fisch and A. H. Boozer, "Creating an asymmetric plasma resistivity with waves," *Physical Review Letters* **45**, 720 (1980).
- ³⁵R. Yoshino, T. Kondoh, Y. Neyatani, K. Itami, Y. Kawano, and N. Isei, "Fast plasma shutdown by killer pellet injection in jt-60u with reduced heat flux on the divertor plate and avoiding runaway electron generation," *Plasma Physics and Controlled Fusion* **39**, 313–332 (1997).
- ³⁶P. Aleynikov and B. Breizman, "Stability analysis of runaway-driven waves in a tokamak," *Nuclear Fusion* **55**, 043014 (2015).
- ³⁷D. A. Spong, W. Heidbrink, C. Paz-Soldan, X. Du, K. Thome, M. Van Zeeland, C. Collins, A. Lvovskiy, R. Moyer, M. Austin, *et al.*, "First direct observation of runaway-electron-driven whistler waves in tokamaks," *Physical Review Letters* **120**, 155002 (2018).
- ³⁸E. Shustin, V. Popovich, and I. Kharchenko, "Transformation of the distribution function of an electron beam during cyclotron interaction with a plasma," Report (Inst. of Radio Physics and Electronics, Erevan, 1970).